



Loading of zinc oxide nanoparticles from green synthesis on the low cost and eco-friendly activated carbon and its application for diazinon removal: isotherm, kinetics and retrieval study

Peyman Pourali^{1,2} · Yousef Rashtbari² · Aylar Behzad² · Ali Ahmadfazeli³ · Yousef Poureshgh² · Abdollah Dargahi^{4,5}

Received: 26 July 2022 / Accepted: 9 January 2023 / Published online: 19 March 2023
Ardabil University of Medical Sciences 2023

Abstract

Diazinon (DZN) has been reported as an important pesticide with wide application in agriculture. The entry of these compounds into water resources has brought serious environmental problems due to their resistance to biodegradation; thus, this study was considered to be done to explore the process of DZN uptake and the influence of effective parameters. The study was performed experimentally and on a laboratory scale. Investigating the structure and morphology of the nanocomposite was done based on different analyses, i.e., FE-SEM, FTIR, and XRD. The experiments based on the Box–Behnken scheme were performed by surveying four important operating parameters (pH, contact time, nanocomposite dose, and DZN concentration). Optimization was performed by experiment design software and using the response surface method and analysis of the proposed model. The DZN removal efficiency was obtained 100% under optimal conditions including pH = 5, nanocomposite dose = 0.83 g/L, reaction time = 55 min, and DZN concentration = 5 mg/L. Considering the high correlation coefficient $R^2 = (0.9873)$ and $R^2_{Adj} = (0.9725)$, the proposed model (quadratic) was approved. The results were indicative of conforming the reaction kinetic to the pseudo-second-order model and the correspondence of reaction isotherm to the Freundlich model ($R^2 = 0.997$). Based on the obtained results, the adsorption process with AC–ZnO nanocomposite could be introduced as an efficient and eco-friendly technique to remove DZN.

Keywords Green synthesis · ZnO nanoparticles · Activated carbon · Oregano extract · Diazinon · Adsorption

Introduction

The increasing expansion of industries and the entrance of industrial and agricultural wastewaters into the environment have been resulted in many concerns about surface water and groundwater pollution and environmental degradation (Janati et al. 2017; Méndez-Paz et al. 2005; Zhang et al. 2005). Wastewater released from pesticide production industries contains high concentrations of pollutants that generally have high toxicity and resistance (Xiong et al. 2011). Organic insecticides include various types such as organochlorines, organophosphates, carbamates, and pyrethroids; one of the most important of them is organophosphate insecticides (Legrouri et al. 2005; Zohair 2001). Diazinon (DZN) as an organophosphate compound has been considered as a promising toxin due to its extensive uses to control a variety of domestic insects, soil insects, pests of fruits and vegetables and agricultural products, home grasses, and the fish parasitic in aquariums as well (Moradiasl et al. 2019; Samadi et al. 2010). This toxin is in the

✉ Yousef Poureshgh
yusef.poureshgh@gmail.com

✉ Abdollah Dargahi
a.dargahi29@yahoo.com

¹ Students Research Committee, Faculty of Health, Ardabil University of Medical Sciences, Ardabil, Iran

² Department of Environmental Health Engineering, School of Public Health, Ardabil University of Medical Sciences, Ardabil, Iran

³ Department of Environmental Health Engineering, School of Health, Tehran University of Medical Sciences, Tehran, Iran

⁴ Department of Environmental Health, Khalkhal University of Medical Sciences, Khalkhal, Iran

⁵ Social Determinants of Health Research Center, Ardabil University of Medical Sciences, Ardabil, Iran

row of "relatively dangerous" of class 2 in the World Health Organization (WHO) classification. The toxicity concentration of this insecticide for marine organisms is 350 ng/L, LC_{50} for killing fishes (48 h) is 4.4 mg/L, and the lethal dose for a human is about 90–444 mg/kg (Videira et al. 2001). DZN, one of broadly used organophosphate insecticides in agriculture uses in worldwide, is released into water sources through direct washing or irrigation. Since most pesticides are used during the spring, they are washed away by rain due to the high rainfall in this season. Moreover, it has been detected that through infiltration of water into soil layers, pesticides can enter groundwater aquifers. Thus, the contamination of water sources can happen through various pathways. Their entry into water supply sources can harmfully affect human health and the environment; the type of chemical, duration of use, time of exposure, the concentration of input toxin, and the degree of toxicity are the factors which control the incident of adverse effects associated with these chemicals (Bazrafshan et al. 2007; Samadi et al. 2010). The final location of most toxins usually leads to rivers, lakes, and lagoons. DZN is relatively soluble in water (40 mg/L at 25 °C), non-polar, sedentary, and resistant in soil. Therefore, it is worrying for ground waters and surface waters that supply drinking water (Liu et al. 2018). Abdominal pain, dizziness, headache, double nose, nausea, and eye and skin problems have been listed as short-term adverse health effects associated with exposure to pesticides by researchers. However, they reported the increase in probability incident of respiratory problems, noted memory disorders, depression, neurological deficits, cancer, and infertility as long-term effects (Samadi et al. 2010). In comparison between dark and light environments, it has been found that the half-life of DZN in the light environment was 31.13 days, while the half-life of the samples kept in the dark was 37.19 days. It decomposes under the influence of UV rays, the amount of which depends on the wavelength used (Hameed et al. 2009). Various methods such as photocatalytic (Ghodsí et al. 2020), biological (Azizi et al. 2021), electrochemical (Heidari et al. 2021; Mahmoudpoor Moteshaker et al. 2020), and ozonation (Arfaeínia et al. 2018) have been utilized for removing DZN from aqueous environments. Chemical oxidation is not dissociated all organic matter, and the biological treatment method is performed at low speed and its sludge disposal faces some problems (Oller et al. 2011). Due to the high-cost and operational problems, the application of mentioned techniques is not cost-effective in many countries. In the meantime, the adsorption method has received more attention since it exhibited characteristics, e.g., easy operation, low investment cost, insensitivity to toxic substances, the possibility of reusing the adsorbent through reduction, and the production of the by-products (Baghapour et al. 2013; Malakotian et al. 2016). Among the used adsorbents, activated carbon (AC), as an extensively used materials in removing organic pollutants from wastewater, has found to be effective since

it has acceptable porosity, specific area and high adsorption capacity, and appropriate efficiency (Pouretedal and Sadegh 2014). Nevertheless, commercial AC has high cost, and due to this problem, studies on low-cost materials for replacing commercial activated carbon are continued by researchers. AC can extensively be obtained from materials, e.g., algae, coconut shell, corn, lignin, etc. Worn tire is widely available in most areas (Mohan and Pittman 2006). Producing activated carbon from worn tire diminishes the risks associated with their disposal and leads to obtain a valuable product (Hoseinzadeh and Rahmani 2012).

A numerous methods have been developed for synthesizing nanoparticles. Because of application of a chemical reducing agent in most chemical methods for controlling the growth of particles and prevention of accumulation, recently incremental attention has been paid to the synthesis of eco-friendly nanoparticles. Biological methods have been introduced as an alternative method for the synthesis of nanoparticles. Conducting biological methods is done using extracts of various plants and their products as an alternative for synthesizing nanoparticles (Fazlzadeh et al. 2017; Ramezani et al. 2013). The critical drawback detected for the employment of nanomaterials in treatment technology is the separation of the dispersed nanocomposites from the aqueous environments at the end of the process. Accelerating the separation of the nanomaterials from the aqueous environments can be done by the stabilization of nanoparticles on materials such as oxides, polymers, fibers, and activated carbon. Among the mentioned cases, the use of activated carbon has shown the economic benefits and environmental considerations (Fazlzadeh et al. 2017; Ghaedi et al. 2013; Samarghandi et al. 2018).

One of the models employed in designing experiments is response surface methodology (RSM); this is a simple, effective, and low-cost method for optimizing various processes (Amouei et al. 2016; Pourali et al. 2022). The Box–Behnken method is a quadratic design based on three-level factorial designs, which is capable of estimating the amount of parameters in a quadratic model and calculating the amount of incompatible parameters by performing the required designs (Ghorbani and Bagherian 2016). In our study, the RSM was applied by applying Box–Behnken model design for optimizing and also evaluating the effect related to independent variables on response performance (DZN removal) and on the other hand predicting the best response value.

Material and methods

Chemicals

Diazinon (DZN, a purity of 0.99) was prepared by Sigma-Aldrich Company, and sodium hydroxide, sulfuric acid

and zinc chloride used were supplied by Merck Company. The physicochemical characteristics of DZN are brought in Table 1. Sulfuric acid and 0.1 M sodium hydroxide were employed for adjusting the solution pH. Maternal solution was used to prepare different concentrations of DZN according to mg/L.

Experiment method

In this experimental research, the efficiency of adsorption process in DZN removal was investigated on a laboratory scale and in a batch system on synthetic wastewater. The sample size used in each step of test is 100 cc. In this design, four parameters of time, nanocomposite content, DZN concentration and solution pH were inspected at three levels, i.e., high (+1), medium (0), and low (−1). The number of required experiments was determined using BBD by formula of $N = 2K(K-1) + C$ (N indicates the number of test samples, K is indicative of the number of variables, and C is representative of the number of center points) (Samarghandi et al. 2021). The number of experiments was 46, which with 13 repetitions of each sample for certifying the accuracy and precision of the results, the number of experiments is 138. Eventually, the samples were withdrawn from solution, and centrifugation was considered for them at 5000 rpm. They were then filtered by applying a filter of 0.22 micron to ensure separation of the nanocomposite. Equation 1 was employed for estimating DZN removal efficiency (%) (Aynaz et al. 2022).

$$\text{Removal efficiency (\%)} = \frac{c_0 - c_e}{c_0} \times 100 \quad (1)$$

C_0 and C_e represent the initial and final DZN concentrations (mg/L). For measuring the concentration of DZN, a spectrophotometer (DR-5000 made by the American company HACH®) was utilized at 247 nm (Dargahi et al. 2021, 2019). After optimizing the operating parameters, the isotherm and kinetics of the process were investigated.

Preparation of powdered activated carbon (AC)

In this study, worn rubber was employed for preparing powdered AC. The first stage of this procedure was impregnation of tire parts (0.5 cm) with phosphoric acid and placing inside a batch reactor. Then, it was placed at 800 °C for 2 h. After washing the prepared AC with distilled water and drying in an oven at 110 °C for 2 h, its separation was done using a sieve [mesh of 20–30 (0.59–0.84 mm)] and considered to be used in our study (Fazlzadeh et al. 2017).

Extraction of plant extract and synthesis of zinc oxide nanoparticles (ZnO)

The obtained Oregano extract was filtered by boiling for 60 min with a vacuum pump. In order to synthesize nanoparticles, $ZnCl_2$ solution was added to the extract in a certain ratio. The appearance of white precipitation indicates the formation of zinc-oxidized nanoparticles. After that, the nanoparticles were dried at 70 °C for 24 h and placed in a kiln at 400 °C for 2 h to calcinate (Fazlzadeh et al. 2017).

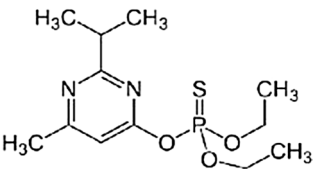
Loading of ZnO nanoparticles onto AC

Preparing the composite was carried out briefly as follows: After adding the ZnO nanoparticles (0.05 g) to distilled water (200 mL), using a magnetic stirrer, the mixture was stirred for 10 min. Then, AC (5 g) was poured into the solution prepared in previous step. After placing it on a magnetic stirrer at 500 rpm for 2 h, loading of the nanoparticles onto the AC was done. After filtering the synthesized composite and rinsing twice with distilled water, it was lastly transferred to the oven at 95 °C for 10 h for complete drying (Rashtbari et al. 2019).

Determination of zero-point pH (pHzpc)

pHzpc indicates the state of electrical charge dispersal on the nanocomposite surface. For determining pHzpc, salt solution of electrolyte (0.1 M), caustic soda (NaOH) and sulfuric acid

Table 1 Physicochemical characteristics of DZN (Ouznadji et al. 2016; Samadi et al. 2010)

Chemical structure	Solubility in water	Molecular formula	Molar mass
	40 mg/L at 25 °C	$C_{12}H_{21}N_2O_3PS$	304.35 g/mol

(H₂SO₄) solutions (0.1 N) were used as controlling agents. 30 ml (in each Erlenmeyer) of the electrolyte solution was poured into 12 of 100 ml Erlenmeyer, and the solution pH was adjusted in the range of 2–12 using H₂SO₄ and NaOH. After adding AC–ZnO nanocomposite (0.05 g) to each Erlenmeyer, they were placed on a shaker at 250 rpm for 48 h. After the termination of the final pH, the contents of the Erlenmeyer were read using a pH meter, after separation of the nanocomposite. pH_{zpc} was estimated by drawing the pH changes curve versus the initial pH (Rivera-Utrilla et al. 2010).

Determination of AC–ZnO nanocomposite specifications

To determine the phase of crystals in AC–ZnO from X-ray diffraction (XRD) at $2\theta = 10\text{--}80^\circ$ by XRD device [model with a PW 3700/30 control X-ray diffraction system (Quanta chrome, NOVA2000, USA)]. The FTIR technique in the range of 450–4000 cm⁻¹ to pinpoint the existing factor group was used on the AC–ZnO surface. FE-SEM scanning electron microscope at an accelerated voltage of 10 keV was the analysis employed for determining the surface and morphological characteristics.

Experiment design based on Box–Behnken

The four studied variables along with their selected levels and amplitudes for the experiment design based on Box–Behnken are presented in Table 2.

Adsorption kinetics

In this section, kinetic equations, which explain how to transport adsorbate per unit of time or to evaluate variables affecting the reaction rate, were employed. Pseudo-first-order (PFO) and pseudo-second-order (PSO) kinetic models were investigated to survey the factors affecting the reaction rate of DZN adsorption process using nanocomposites. The PFO and PSO linear kinetic equations are stated in form of Eqs. (2) and (3), respectively (Pourali et al. 2021):

$$\ln(q_e - q_t) = \ln q_e - k_1 t \quad (2)$$

$$\frac{t}{q_t} = \frac{1}{K_2 q_e^2} + \frac{1}{q_e} t \quad (3)$$

In mentioned equations, K_1 and K_2 are the velocity coefficient (1/min) and the PSO reaction constant (mg/g min), respectively. q_e and q_t are the adsorption capacity at equilibrium time and t time (mg/g), respectively. Moreover, q_e and K_1 values are y-intercept and the slope of the line resulting from drawing $\ln(q_e - q_t)$ versus t , respectively. In Eq. (3), determining the values of q_e and K_2 are done based on the slope and y-intercept of the linear graph of t/q_t versus t (Abdollahzadeh et al. 2022; Kakavandi et al. 2013).

Adsorption isotherms

This section was done based on adsorption isotherms. They have been defined as adsorption properties and equilibrium data; these are utilized for describing the quality of contaminants' reaction with nanocomposite materials and exhibit effective participation in optimizing the consumption of nanocomposites (Hii et al. 2009). Langmuir's model comprises hypotheses such as surface uniformity, monolayer adsorption, and eliminating the interaction of adsorbed molecules. The equation of the mentioned model is the monolayer adsorption process as follows:

$$\frac{C_{eq}}{q_{eq}} = \frac{1}{Qb} + \frac{C_{eq}}{Q} \quad (4)$$

$$R_L = \frac{1}{1 + bc} \quad (5)$$

In cited equations, q_e (mg/g) has been used to show the quantity of absorbed DZN per gram of nanocomposite, and C_e (mg/L) was employed to represent the equilibrium DZN concentration in equilibrium. Langmuir parameters were represented by Q and b ; these indicate maximum adsorption capacity and adsorption correlation energy, respectively (Eq. 4) (Biglari et al. 2018). One of the properties of the mentioned equation employed for determining the type of adsorption process is the dimensionless parameter of the separation coefficient R_L (Eq. 5); for $R_L > 1$, $R_L = 1$, $0 < R_L < 1$, and $R_L = 0$, adsorption is undesirable, linear, desirable, and irreversible, respectively (Shu et al. 2020; Zhang et al. 2019). When the adsorption sites are uniform and the surface is monotonous, the Langmuir relationship is consistent with empiric experiments, but if the surface is heterogeneous, the Freundlich relationship which has obtained by measuring the amount of adsorbed material at different pressures provides a superior description of the data. The Freundlich model of the adsorption process is defined by Eq. (6):

Table 2 Selected levels and code for Box–Behnken test design

Variable	Sign	Unit	Levels		
			-1	0	+1
Initial pH of the solution	A	–	3	7	11
Nanocomposite value	B	g/L	0.2	0.6	1
Contact time	C	min	10	35	60
Initial concentration of DZN	D	mg/L	5	30	55

$$\log(q_e) = \log(K_f) + \frac{1}{n} \log(C_e) \quad (6)$$

C_e was used to represent equilibrium concentration in mg/L and q_e is absorption capacity at equilibrium time in mg/g. and Freundlich absorption constants were shown by K_f and n ; these represent the capacity and intensity of adsorption (Kaushal et al. 2018). In this model, values of n are less than an indicator of weak absorption, and observing the values of 1–2 and 2–10 are representative of moderate and desirable absorption, respectively (Hao et al. 2010). The values of n and K_f coefficients are determined by the slope and y-intercept of the linear graph $\log(q_e)$ versus $\log(C_e)$, respectively.

Result and discussion

Investigation of the structural nature of nanocomposite

XRD analysis

In Fig. 1, the X-ray patterns obtained for AC–ZnO nanocomposites have been detected. Considering its results, the peaks created at 31.75, 34.45, 36.32, 47.52, 59.6, 62.85, 66.45, 67.95 and 69.15° are indexes of the structure of ZnO. In addition, appearing sharp and elongated peaks at angles of 23, 24.43, 27.33, 28.93 and 42° was related to the existing carbon in the activated carbon structure. The peak $2\theta = 16$ is attributed to the residual NaOH (Ai et al. 2010; Rashtbari et al. 2020a; Xu et al. 2017).

FTIR analysis

As perceived by the FTIR spectrum (Fig. 2), the position of most of the bands in the nanocomposite structure remains unchanged after loading the nanoparticles which

indicates the preservation of the structure of the nanocomposite. The absorption peak at 900–1300 cm^{-1} corresponds to functional groups containing phosphorus that is related to the activation of nanocomposites using phosphoric acid during the preparation process (Afshina et al. 2021). The peaks below 700 cm^{-1} are related to the vibrations of the Zn–O bonds. The presence of ZnO nanoparticles can be demonstrated by appearing a strong adsorption band at 598–626 cm^{-1} . The band corresponding to 3444 cm^{-1} is linked to the O–H vibration in the H_2O molecule. A peak in the range of 2921–2948 cm^{-1} indicates the effect of C–H and O–H (with acid origin) in the Oregano extract for the formation of nanoparticles. Polyphenols act as the foremost stabilizing agent for NPs, ranging from 1300 to 3500 cm^{-1} (Rashtbari et al. 2020c). The C=O (carboxylic) groups are in 1540–1750 cm^{-1} and the aromatic group of C=C is in 1450–1600 cm^{-1} (Shahrokhi-Shahraki et al. 2021).

Morphology of AC–ZnO nanocomposite using FE-SEM analysis

Figure 3a shows ZnO nanoparticles. As shown in the figure, the agglomeration of some nanoparticles together and their precipitation during the heating process are detected; this also indicates the morphology of ZnO particles with a spherical nanosphere size (Gojarati et al. 2020). The approximate particle size distribution was obtained as about 21 nm. In Fig. 3b, it is seen that stabilizing ZnO nanoparticles on AC partially blocks the porosity of activated carbon, probably because ZnO nanoparticles cannot enter the internal cavities of activated carbon, which is led to remain on the outer surface of activated carbon and cavities with smaller sizes remain intact. The white particles shown in Fig. 3b on activated carbon indicate the existence of ZnO on the powdered activated carbon

Fig. 1 XRD spectrum for AC–ZnO nanocomposite

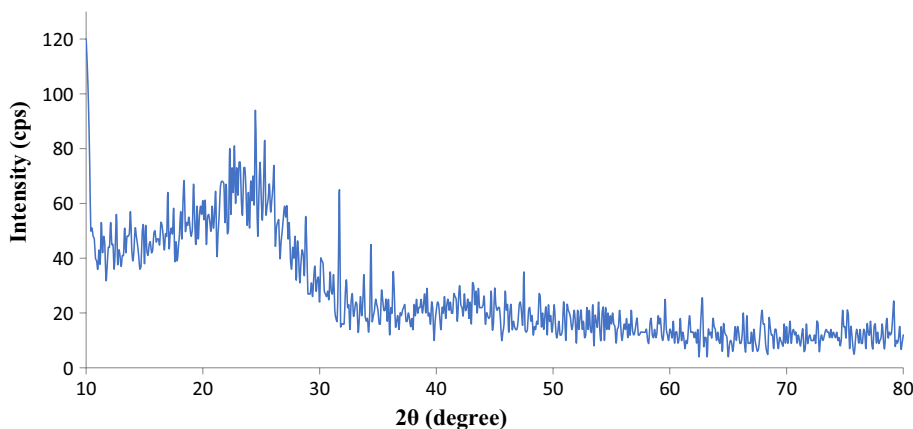


Fig. 2 FTIR spectrum for ZnO and AC-ZnO nanocomposite

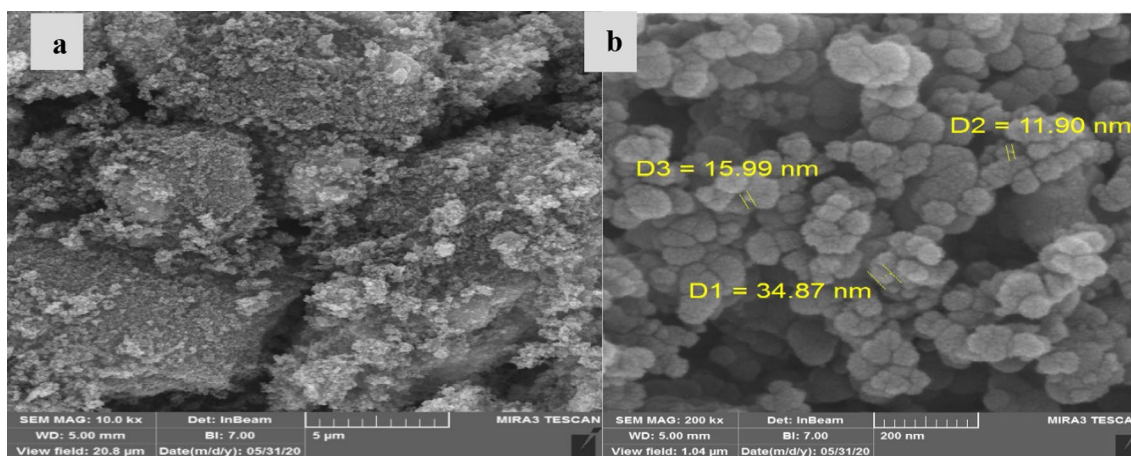
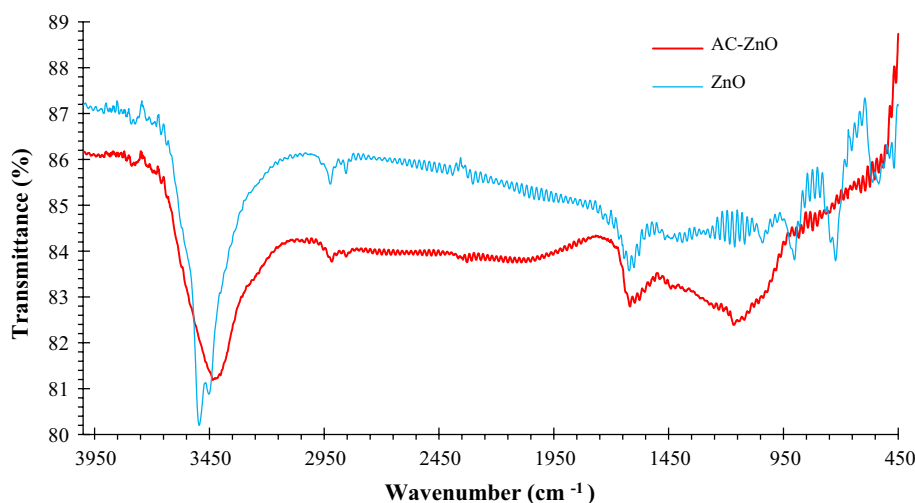


Fig. 3 FE-SEM pattern: ZnO (a) AC-ZnO nanocomposite (b)

surface and its proper stabilization (Afshin et al. 2020; Rashtbari et al. 2020c).

Fitting quadratic polynomial model and statistical analysis

Presentation of quadratic polynomial model and ANOVA analysis

Considering the Box-Behnken scheme, a quadratic polynomial equation was obtained to represent the empirical relationship between experimental results and input variables, which is epitomized based on coded factors as follows:

$$Y = + 87.6 - 18.67 A + 5.7 B - 16.34 C + 6.12 D + 1.28 AB + 0.295 AC + 1.26 AD + 2.43 BC + 238 + 3.63 BD + 2.83 CD - 26.04 A^2 - 4.94 B^2 - 5.18 C^2 - 3.05 D^2$$

In above equation, *Y* has been employed to show the removal rate (%), and *A*, *B*, *C* and *D* are utilized to symbolize the pH, nanocomposite, time, and initial concentration, respectively. Considering ANOVA analysis (Table 3), statistically significant relationship could be detected for the proposed model with linear conditions according to one-way variance analysis ($p \leq 0/001$). In addition, completely significant interaction was seen between *A*, *B*, *C* and *D* parameters and B^2 ($p \leq 0/001$). For this model, the value of *F* has been 500.71; this means the significant variance of each variable compared to the error variance and effective role of all the main parameters as a response (Heidari et al. 2021; Rashtbari et al. 2021). pH with $F = 2251.67$ is the

Table 3 Variance analysis of operational parameters in DZN adsorption

Source	Sum of squares	df	Mean square	F-value	p value	
<i>Model</i>	13026.65	14	930.47	500.71	< 0.0001	Significant
A-pH	4184.32	1	4184.32	2251.67	< 0.0001	
B-dose	390.11	1	390.11	209.93	< 0.0001	
C-conc	3201.99	1	3201.99	1723.06	< 0.0001	
D-time	448.96	1	448.96	241.60	< 0.0001	
AB	6.55	1	6.55	3.53	0.0800	
AC	0.3481	1	0.3481	0.1873	0.6713	
AD	6.30	1	6.30	3.39	0.0854	
BC	23.57	1	23.57	12.68	0.0028	
BD	52.64	1	52.64	28.32	< 0.0001	
CD	31.98	1	31.98	17.21	0.0009	
A ²	4650.74	1	4650.74	2502.67	< 0.0001	
B ²	167.03	1	167.03	89.88	< 0.0001	
C ²	183.67	1	183.67	98.84	< 0.0001	
D ²	63.81	1	63.81	34.34	< 0.0001	
<i>Residual</i>	27.87	15	1.86			
Lack of fit	19.66	10	1.97	1.20	0.4463	Not significant
Pure error	8.21	5	1.64			
<i>Cor total</i>	13,054.52	29				

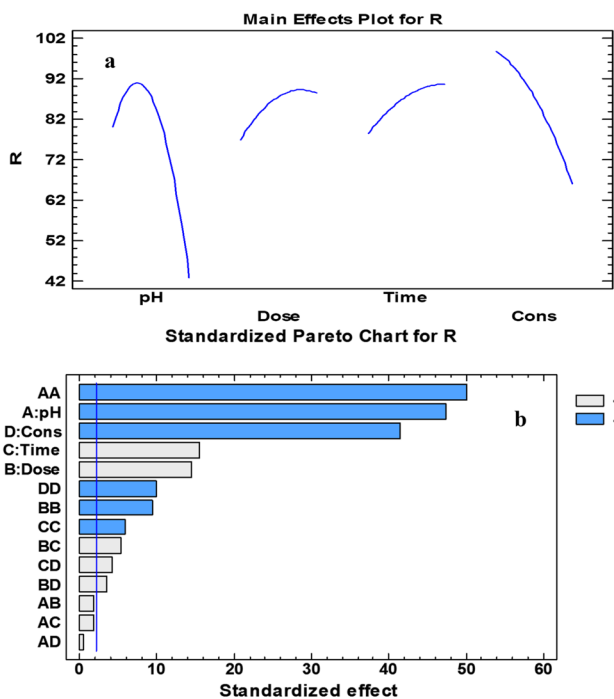


Fig. 4 Initial effect of considered parameters (a), effect of all factors on DZN removal (b)

most effective factor in DZN uptake process. In addition, the adjusted correlation coefficient (R^2_{adj}) equal to 0.9723 is representative of the high accuracy of the statistical model. Figure 4a discloses the effective variables considered for

DZN removal (reaction time, pH, nanocomposite dose and initial DZN concentration). The range and selectivity of the variables, the amount of impact and the optimal points of each variable can also be seen in this figure. Based on the Pareto diagram in Fig. 4b, the most negative effects were related to pH and concentration, respectively. Also, the most positive effects were related to the reaction time and nanocomposite mass in removing DZN, respectively.

Checking the accuracy and validity of the proposed model

In the statistical analysis of experimental data, it is necessary to check that the data have a normal distribution, in the normal distribution, the points of the data are very close to each other and they follow a straight line that is descending (Almasi et al. 2016; Dargahi et al. 2022). The normal probability diagram (Fig. 5a) has shown to determine how the data distribution. The represented diagram clearly illuminates a reasonable normal distribution of data related to DZN adsorption. Validating the proposed model was done based on various analyses. Considering graph generated by drawing experimental data versus the predicted data by the model of Fig. 5b, the uniformity and consistency of values along a straight line are detected and have a high correlation (Ponnusami et al. 2007).

Effect of soluble pH

One of the important controlling factors in this type of research is the solution pH. Figure 6a discloses the effect of

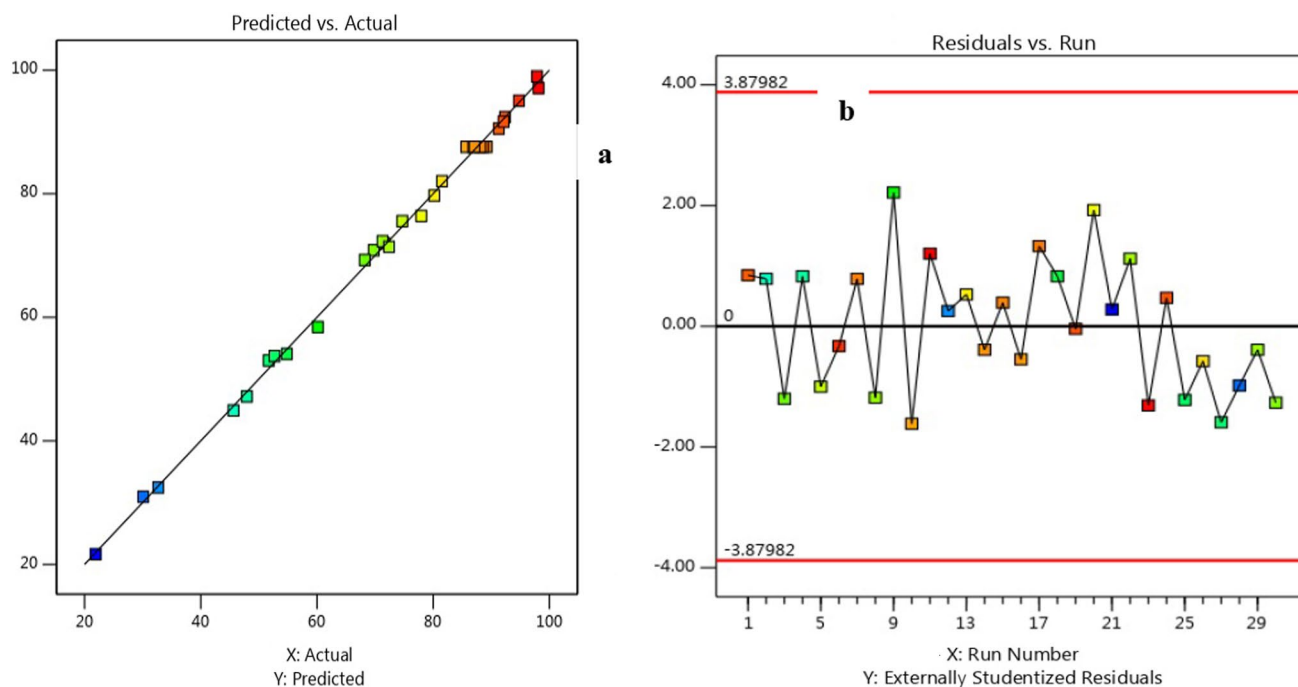


Fig. 5 Normal probability (a), fitting experimental data versus predicted data (b)

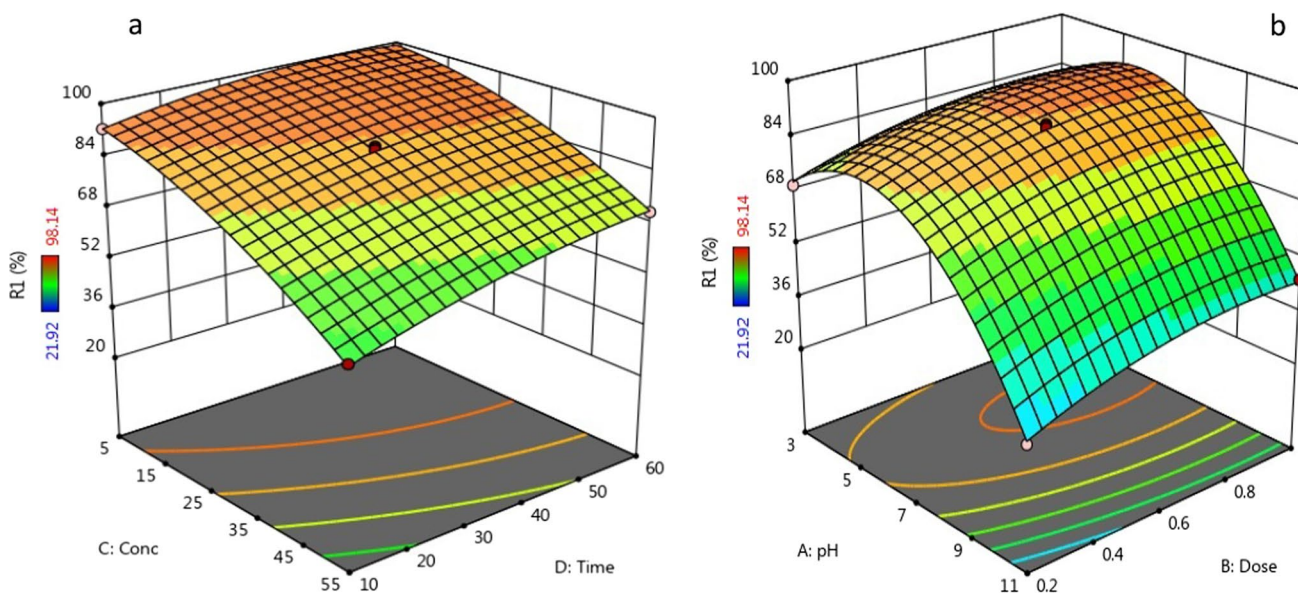


Fig. 6 Effect of changes in variables on DZN adsorption efficiency: **a** Nanocomposite and pH value (initial concentration of 30 mg/L, contact time 35 min), **b** initial concentration and contact time (pH = 7, nanocomposite value = 0.6 g/L)

mentioned parameter on the DZN removal. As shown in the figure, our pH range in this study was 3–11, and the highest and lowest amount of DZN uptake was seen at the pH of 5 and 11, respectively. Since the evaluated parameter is very influential on the adsorption process through the speciation charge of the nanocomposite material, the surface charge of the nanocomposite, and the degree of ionization, based on

the point of zero charge (pH_{zpc}), at a pH higher than pH_{zpc} , the dominant surface electric charge on the surface of the nanocomposite is a negative charge, and at pH lower than pH_{zpc} , the dominant surface charge on its surface is positive. The noted characteristic of nanocomposites has been recognized as a principle for inferring and defining the mechanism of the adsorption process (Ouazene and Sahmoune 2010).

In our study, the pH_{zpc} value was higher than the optimum pH value, which causes the electrostatic adsorption of DZN molecules to be dissociated anionically in an acidic solution. Electrostatic repulsion reduced the adsorption of anionic DZN (Armaghan and Amini 2009; Moussavi et al. 2013). Therefore, DZN uptake may be associated with an increase in negative charge at the nanocomposite surface (Moussavi et al. 2013; Zolgharnein et al. 2013). Our observations were consistent with the reports of Esfandian et al. (2016).

Effect of nanocomposite dose

The nanocomposite dose range in this study was between 0.2 and 1 g/L, the highest DZN uptake efficiency arisen at the nanocomposite mass of 0.83 g/L. Based on Fig. 6a, the adsorption efficiency has increased by raising the amount of used nanocomposite. It is readily available that the active adsorption sites increase by increasing nanocomposite mass in solution. Determination of nanocomposite mass is a most important issue in adsorption systems due to economic considerations (Fazlzadeh et al. 2016). Although raising the nanocomposite dose increases the removal of DZN, it leads to reduce the adsorption capacity. The diminution in capacity might be described as follows: Increasing the nanocomposite mass for a constant concentration and volume of solution will lead to saturating the active sites of the nanocomposite during the studied process. Moreover, it may also be related to the interaction between particles such as the particles caused by the high concentration of nanocomposites (Jesus et al. 2011; Rashtbari et al. 2020b). The increase in DZN removal percentage is due to greater access to adsorption sites. It may also be explained based on the raise of ion exchange sites on the nanocomposite surface, which develops the dye bonding to the nanocomposite surface (Bazrafshan et al. 2014; Haghighi et al. 2016). Our results exhibited a consistency with Hung et al. (Shu et al. 2007).

The effect of DZN concentration

Contaminant concentration is a central and influential factor in the adsorption process. In this study, the initial concentration in the range of 5–55 mg/L was studied, and 5 mg/L was obtained as the optimal concentration. Figure 6a shows that the adsorption efficiency is associated with a decline for higher DZN concentration. Saturating the nanocomposite surface at high DZN concentrations was the main reason for the observed dwindling trend. Furthermore, at high concentrations, there will be larger amounts of remaining DZN ions in a certain volume of the unabsorbed solution, and as a result, the DZN removal diminishes in

the solution. In contrast, for low concentrations of DZN, the ratio of DZN to the nanocomposite surface was low. Therefore, the DZN ion adsorption is effortlessly happened by active sites, and DZN ion removal enhances (Ouznadji et al. 2016; Rashtbari et al. 2022). Our study represented results similar to the study of Dehghani et al. (2019).

The effect of contact time

To study the effect of reaction time on eliminating DZN, a contact time in the range of 10–60 min was selected. Examination of mentioned parameter effect on DZN removal by nanocomposite in Fig. 6b disclosed that raising contact time develops the removal rate so that the maximum removal for DZN occurred at 55 min. Considering Fig. 6b, a rapid enhancement in DNZ removal is recognized at the beginning of the adsorption process; existing high unsaturated active sites on the outer surface of the nanocomposite describe the mentioned event (Liu et al. 2018; Saeidi et al. 2016). After a while, the repulsion between the DZN molecules in the solid and liquid phases leads to difficulty in occupying the remaining empty surface spaces (El Bakouri et al. 2009; Hameed et al. 2009; Moussavi et al. 2013). Our results were detected to be in agreement with the results reported by Dehghani et al. (2019).

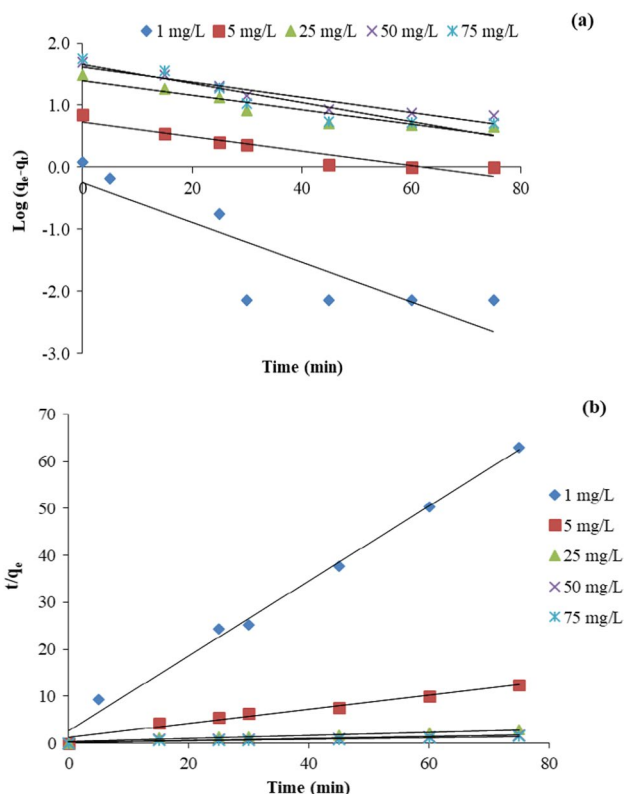


Fig. 7 Pseudo-first (a) and second-order (b) kinetic model in DZN adsorption using AC-ZnO composite

The studies of isotherm and adsorption kinetics

Figure 7 shows the pseudo-first-order (PFO) and second-order (PSO) kinetic models, respectively. Considering mentioned figure, the fit of the experimental data to the PSO with the regression coefficient ($R^2=0.99$) has been associated with a superior compared to the PFO. Also, the predicted equilibrium adsorption capacity by the PSO differs less from the experimental value of the equilibrium adsorption capacity than the PFO. The parameters of the PFO and PSO are publicized in Table 4; based on this figure, the rate constant of the PSO equation (K_2) declines by increasing DZN concentration. Since there are enough sites in a fixed amount of nanocomposite to adsorb lower concentrations of DZN, a tendency to reduce K_2 is detected, which enhanced the rate of adsorption. However, a gradual decline in the adsorption rate of soluble substances is perceived later, which corresponds to the reduction of active sites required for high concentrations of DZN, (Nikzad et al. 2019).

To draw the utilized isotherms in our research, adsorption experiments were performed on pH, nanocomposite dose, and optimal contact time. Finally, adsorption isotherms were plotted for both models based on laboratory data and gotten parameters from linear regression. Considering Fig. 8 and Table 5, the DZN adsorption using AC–ZnO nanocomposite follows the Freundlich isotherm model ($R^2=0.997$). Accordingly, the Freundlich model shows an enhanced fit and is able to well define the DZN adsorption behavior; therefore, the results are indicative of the uniform scattering of active sites on the nanocomposite surface and subsequently occurring DZN adsorption on homogeneous locations. The results completely correspond with the reports represented in other similar documents (Amarathunga and Mathota Arachchige 2020; Farhadi et al. 2021).

According to Table 6, which has been represented for comparing the adsorption capacity detected for employed adsorbents in earlier studies for eliminating DZN, the adsorption capacity of DZN using AC–ZnO nanocomposite found in our research was superior compared to the other nanocomposites. AC–ZnO nanocomposite has been recognized as an apt, inexpensive, and eco-friendly adsorbent since it exhibited a high adsorption capacity in DZN adsorption.

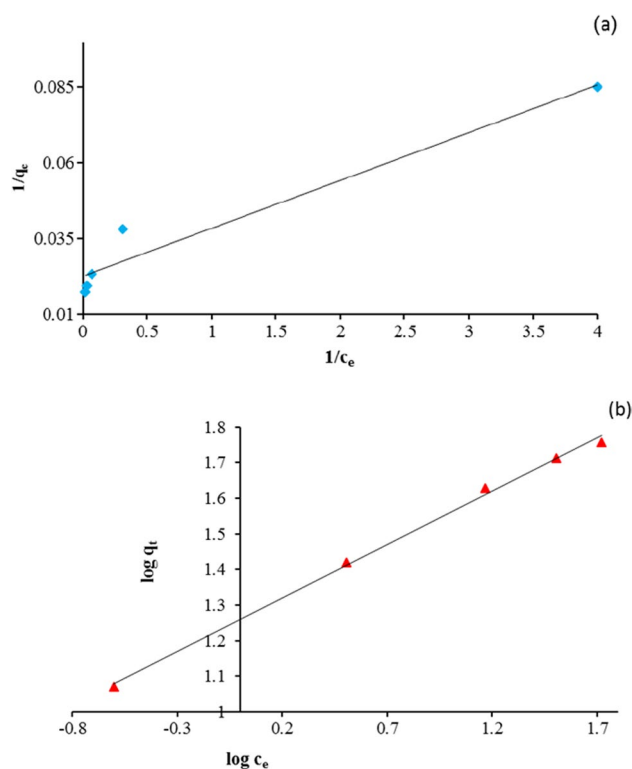


Fig. 8 Langmuir (a) and Freundlich (b) isotherm model in DZN adsorption using AC–ZnO nanocomposite

Conclusion

Considering this study, the notable effective synthesis of AC–ZnO nanocomposite was confirmed so that the DZN elimination from aqueous environments at the studied range of concentrations was successfully done by this nanocomposite. It is also revealed that by raising the time and the nanocomposite mass, the process could offer more preferable results, and in contrast, raising the initial DZN concentration decreases the adsorption efficiency. Considering isotherm and kinetics analysis, the data follow the Freundlich model and PSO kinetics. A high adsorption capacity (based on Langmuir model) of 44 mg/g was detected for this nanocomposite. Using optimal conditions (initial DZN concentration = 5 mg/L,

Table 4 Calculated variables for kinetic models

C_0 (mg/L)	Pseudo-first-order				Pseudo-second-order			
	$q_{e,exp}$ (mg/g)	$q_{1,cal}$ (mg/g)	k_1 (1/min)	R_1^2	$q_{2,cal}$ (mg/g)	K_2 (g mg/min)	R_2^2	
1	1.2	1.77	0.0736	0.7481	1.25	0.2497	0.9932	
5	7	5.38	0.0269	0.8985	6.59	0.0192	0.9678	
25	31	25.14	0.0271	0.8902	30.12	0.003	0.9342	
50	50	41.43	0.0281	0.9162	49.26	0.0017	0.9294	
75	57	45.49	0.0352	0.8673	60.24	0.0014	0.9087	

Table 5 Parameters of Langmuir and Freundlich isotherm model

Pollutant	Langmuir isotherm				Freundlich isotherm		
	q_m (mg/g)	K_l (L/mg)	R^2	R_L	K_f [(mg/g) (mg/L) $^{1/n}$]	n	R^2
DZN	44.05	1.43	0.9516	0.06	18.18	3.33	0.997

Table 6 Comparison of maximum absorption capacity (q_{max}) of different nanocomposites for DZN absorption

Type of nanocomposite	pH	q_{max} (mg/g)	References
AC–ZnO	5	44	Current study
Loess	5.6	24.69	Ryoo et al. (2013)
Montmorillonite	7	16.5	Nikzad et al. (2019)
Coconut shell-modified biochar	3	10.33	Baharum et al. (2020)
Bentonite	5.2	5.56	Ouznadji et al. (2016)
MCM-41	9	5.16	Amani et al. (2018)
Organo-zeolite	7	1.35	Lemić et al. (2006)

nanocomposite mass = 0.83 g/L, time = 55 min, and pH = 5), the process efficacy was about 100%. Overall, AC–ZnO nanocomposite was introduced as high efficient and accessible, eco-friendly, and inexpensive adsorbent for removing DZN from industrial wastewater; this was obtained by careful surveying of the operating conditions of the adsorption process.

Acknowledgements I warmly express honorable deputy of Research and Technology of Ardabil University of Medical Sciences and Health Services appreciation due to financial support of this research (with project code of IR.ARUMS.REC.1398.638).

Author contributions All authors had equal contributions in writing, review, and final approval of the paper.

Funding Funding was supported by Ardabil University of Medical Sciences (Grant No. IR.ARUMS.REC.1398.638).

Data availability The dataset and analyzed during the current study are available from the corresponding authors on realistic demand.

Declarations

Conflict of interest The authors declare that there is no conflict of interest regarding the publication of this work.

Ethical approval Not applicable.

Consent for publication Not applicable.

Consent to participate Not applicable.

Open Access This article is licensed under a Creative Commons Attribution 4.0 International License, which permits use, sharing, adaptation, distribution and reproduction in any medium or format, as long as you give appropriate credit to the original author(s) and the source, provide a link to the Creative Commons licence, and indicate if changes were made. The images or other third party material in this article are included in the article's Creative Commons licence, unless indicated

otherwise in a credit line to the material. If material is not included in the article's Creative Commons licence and your intended use is not permitted by statutory regulation or exceeds the permitted use, you will need to obtain permission directly from the copyright holder. To view a copy of this licence, visit <http://creativecommons.org/licenses/by/4.0/>.

References

- Abdollahzadeh H, Fazlzadeh M, Afshin S, Arfaeinia H, Feizizadeh A, Poureshgh Y, Rashtbari Y (2022) Efficiency of activated carbon prepared from scrap tires magnetized by Fe₃O₄ nanoparticles: characterisation and its application for removal of reactive blue19 from aquatic solutions. *Int J Environ Anal Chem* 102(8):1911–1925
- Afshin S, Rashtbari Y, Ramavandi B, Fazlzadeh M, Vosoughi M, Mokhtari SA, Shirmardi M, Rehman R (2020) Magnetic nanocomposite of filamentous algae activated carbon for efficient elimination of cephalexin from aqueous media. *Korean J Chem Eng* 37(1):80–92
- Afshina S, Poureshgha Y, Rashtbaria Y, Fazlzadehb M, Aslc FB, Hamzezadeha A, Pormazard SM (2021) Eco-friendly cost-effective approach for synthesis of ZnO nanoparticles and loaded on worn tire powdered activated carbon as a novel adsorbent to remove organic dyes from aqueous solutions: equilibrium, kinetic, regeneration and thermodynamic study. *Desalin Water Treat* 227:391–403
- Ai L, Huang H, Chen Z, Wei X, Jiang J (2010) Activated carbon/CoFe₂O₄ composites: facile synthesis, magnetic performance and their potential application for the removal of malachite green from water. *Chem Eng J* 156(2):243–249
- Almasi A, Dargahi A, Mohammadi M, Azizi A, Karami A, Baniamerian F, Saeidimoghadam Z (2016) Application of response surface methodology on cefixime removal from aqueous solution by ultrasonic/photooxidation. *Inte J Pharm Technol* 8(3):16728–16736
- Amani M, Latifi A, Tahvildari K, Karimian R (2018) Removal of diazinon pesticide from aqueous solutions using MCM-41 type materials: isotherms, kinetics and thermodynamics. *Int J Environ Sci Technol* 15(6):1301–1312
- Amarathunga N, Mathota Arachchige Y (2020) Removal of diazinon pesticide from water using a polyacrylamide-Strychnos potatorum (Ingini) seeds derived activated carbon composite. *Faculty of Science, University of Kelaniya, Sri Lanka*, p 104
- Amouei A, Asgharnia H, Karimian K, Mahdavi Y, Balarak D, Ghasemi S (2016) Optimization of dye reactive orange 16 (RO16) adsorption by modified sunflower stem using response surface method from aqueous solutions. *J Rafsanjan Univ Med Sci* 14(10):813–826
- Arfaeinia H, Rezaei H, Sharafi K, Moradi M, Pasalari H, Hashemi SE (2018) Application of ozone/magnetic graphene oxide for degradation of Diazinon pesticide from aqueous solutions. *Desalin Water Treat* 107:127–135
- Armaghan M, Amini MM (2009) Adsorption of diazinon and fenitrothion on MCM-41 and MCM-48 mesoporous silicas from non-polar solvent. *Colloid J* 71(5):583–588

- Aynaz M, Dalia A, Mehdi V, Abdollah D, Amir M (2022) Synthesis of magnetic Fe₃O₄/activated carbon prepared from banana peel (BPAC@Fe₃O₄) and salvia seed (SSAC@Fe₃O₄) and applications in the adsorption of basic blue 41 textile dye from aqueous solutions. *Appl Water Sci*. <https://doi.org/10.1007/s13201-022-01622-6>
- Azizi A, Dargahi A, Almasi A (2021) Biological removal of diazinon in a moving bed biofilm reactor—process optimization with central composite design. *Toxin Rev* 40(4):1242–1252
- Baghapour MA, Jahed B, Joshani G (2013) Preparation of activated carbon from waste tires and its application in gasoline removal from water. *Iranian J Health Environ* 6(3):pe378–pe393
- Baharum NA, Nasir HM, Ishak MY, Isa NM, Hassan MA, Aris AZ (2020) Highly efficient removal of diazinon pesticide from aqueous solutions by using coconut shell-modified biochar. *Arab J Chem* 13(7):6106–6121
- Bazrafshan E, Mahvi A, Nasserli S, Shaieghi M (2007) Performance evaluation of electrocoagulation process for diazinon removal from aqueous environments by using iron electrodes. *J Environ Health Sci Eng* 4(2):127–132
- Bazrafshan E, Zarei AA, Nadi H, Zazouli MA (2014) Adsorptive removal of Methyl Orange and Reactive Red 198 dyes by morning peregriana ash. *Indian J Chem Technol* 21:105–113
- Biglari H, RodríguezCouto S, Khaniabadi YO, Nourmoradi H, Khoshgoftar M, Amrane A, Vosoughi M, Esmaeili S, Heydari R, Mohammadi MJ (2018) Cationic surfactant-modified clay as an adsorbent for the removal of synthetic dyes from aqueous solutions. *Int J Chem Reactor Eng*. <https://doi.org/10.1515/ijcre-2017-0064>
- Dargahi A, Moradi M, Marafat R, Vosoughi M, Mokhtari SA, Hasani K, Asl SM (2021) Applications of advanced oxidation processes (electro-Fenton and sono-electro-Fenton) for degradation of diazinon insecticide from aqueous solutions: optimization and modeling using RSM-CCD influencing factors, evaluation of toxicity, and degradation pathway. *Biomass Convers Biorefinery*. <https://doi.org/10.1007/s13399-021-01753-x>
- Dargahi A, Samarghandi MR, Vaziri Y, Ahmadidoost G, Ghahramani E, Shekarchi AA (2019) Kinetic study of the photocatalytic degradation of the acid blue 113 dye in aqueous solutions using zinc oxide nanoparticles immobilized on synthetic activated carbon. *J Adv Environ Health Res* 7(2):75–85
- Dargahi A, Vosoughi M, Mokhtari SA, Vaziri Y, Alighadri M (2022) Electrochemical degradation of 2, 4-Dinitrotoluene (DNT) from aqueous solutions using three-dimensional electrocatalytic reactor (3DER): degradation pathway, evaluation of toxicity and optimization using RSM-CCD. *Arab J Chem* 15(3):103648
- Dehghani MH, Kamalian S, Shayeghi M, Yousefi M, Heidarinejad Z, Agarwal S, Gupta VK (2019) High-performance removal of diazinon pesticide from water using multi-walled carbon nanotubes. *Microchem J* 145:486–491
- El Bakouri H, Usero J, Morillo J, Rojas R, Ouassini A (2009) Drin pesticides removal from aqueous solutions using acid-treated date stones. *Biores Technol* 100(10):2676–2684
- Esfandian H, Samadi-Maybodi A, Parvini M, Khoshandam B (2016) Development of a novel method for the removal of diazinon pesticide from aqueous solution and modeling by artificial neural networks (ANN). *J Ind Eng Chem* 35:295–308
- Farhadi S, Sohrabi MR, Motiee F, Davallo M (2021) Organophosphorus diazinon pesticide removing from aqueous solution by zero-valent iron supported on biopolymer chitosan: RSM optimization methodology. *J Polym Environ* 29(1):103–120
- Fazlzadeh M, Abdoallahzadeh H, Khosravi R, Alizadeh B (2016) Removal of acid black 1 from aqueous solutions using Fe₃O₄ magnetic nanoparticles. *J Mazandaran Univ Med Sci* 26(143):174–186
- Fazlzadeh M, Khosravi R, Zarei A (2017) Green synthesis of zinc oxide nanoparticles using peganum harmala seed extract, and loaded on peganum harmala seed powdered activated carbon as new adsorbent for removal of Cr (VI) from aqueous solution. *Ecol Eng* 103:180–190
- Ghaedi M, Ghayedi M, Kokhdan SN, Sahraei R, Daneshfar A (2013) Palladium, silver, and zinc oxide nanoparticles loaded on activated carbon as adsorbent for removal of bromophenol red from aqueous solution. *J Ind Eng Chem* 19(4):1209–1217
- Ghods S, Esrafil A, Kalantary RR, Gholami M, Sobhi HR (2020) Synthesis and evaluation of the performance of g-C₃N₄/Fe₃O₄/Ag photocatalyst for the efficient removal of diazinon: kinetic studies. *J Photochem Photobiol A* 389:112279
- Ghorbani M, Bagherian A (2016) Optimization of astrazon blue adsorption onto sulfonated styrene-co-divinylbenzene resin by experimental design methodology. *Nashrieh Shimi Va Mohandesi Shimi Iran* 35(1):25–37
- Gojartati SS, Hajisafari M, Khosravirad MM (2020) Study of photocatalytic activity of zinc oxide nanoparticles extracted from leaching residue of zinc melting factory to remove NB21 dye in UV light. *J Water Wastewater* 31(4):87–98
- Haghighi M, Rahmani F, Dehghani R, MAZAHARI, T.A. and MIRANZADEH, M. (2016) Efficient photocatalytic reduction Of Cr (Vi) over immobilized ZnO nanocrystals under UV light illumination: synergetic effect of Hzsm-5 zeolite as support. *J Appl Chem* 10(3):5–16
- Hameed B, Salman J, Ahmad A (2009) Adsorption isotherm and kinetic modeling of 2,4-D pesticide on activated carbon derived from date stones. *J Hazard Mater* 163(1):121–126
- Hao Y-M, Man C, Hu Z-B (2010) Effective removal of Cu (II) ions from aqueous solution by amino-functionalized magnetic nanoparticles. *J Hazard Mater* 184(1–3):392–399
- Heidari M, Vosoughi M, Sadeghi H, Dargahi A, Mokhtari SA (2021) Degradation of diazinon from aqueous solutions by electro-Fenton process: effect of operating parameters, intermediate identification, degradation pathway, and optimization using response surface methodology (RSM). *Sep Sci Technol* 56(13):2287–2299
- Hii S-L, Yong S-Y, Wong C-L (2009) Removal of rhodamine B from aqueous solution by sorption on *Turbinaria conoides* (Phaeophyta). *J Appl Phycol* 21(5):625–631
- Hoseinzadeh E, Rahmani A (2012) Producing activated carbon from scrap tires by thermo-chemical method and evaluation its efficiency at removal acid black 1 dye. *Iranian J Health Environ* 4(4):427–438
- Janati A, Amini A, Adham D, Naseriasl M (2017) Referral system in Iran's health sector and world's leading countries. *Res J Pharm Technol* 10(6):1597–1602
- Jesus A, Romão L, Araújo B, Costa A, Marques J (2011) Use of humin as an alternative material for adsorption/desorption of reactive dyes. *Desalination* 274(1–3):13–21
- Kakavandi B, Rezaei Kalantary R, Esrafil A, Jonidi Jafari A, Azari A (2013) Isotherm, kinetic and thermodynamic of Reactive blue 5 (RB5) dye adsorption using Fe₃O₄ nanoparticles and activated carbon magnetic composite. *J Color Sci Technol* 7(3):237–248
- Kaushal S, Badru R, Kumar S, Kaur H, Singh P (2018) Efficient removal of cationic and anionic dyes from their binary mixtures by organic-inorganic hybrid material. *J Inorg Organomet Polym Mater* 28(3):968–977
- Legrouiri A, Lakraimi M, Barroug A, De Roy A, Besse J (2005) Removal of the herbicide 2,4-dichlorophenoxyacetate from water

- to zinc–aluminium–chloride layered double hydroxides. *Water Res* 39(15):3441–3448
- Lemić J, Kovačević D, Tomašević-Čanović M, Kovačević D, Stanić T, Pfordner R (2006) Removal of atrazine, lindane and diazinon from water by organo-zeolites. *Water Res* 40(5):1079–1085
- Liu G, Li L, Huang X, Zheng S, Xu X, Liu Z, Zhang Y, Wang J, Lin H, Xu D (2018) Adsorption and removal of organophosphorus pesticides from environmental water and soil samples by using magnetic multi-walled carbon nanotubes@ organic framework ZIF-8. *J Mater Sci* 53(15):10772–10783
- Mahmoudpoor Motesaker P, Saadi S, Rokni SE (2020) Electrochemical removal of diazinon insecticide in aqueous solution by Pb/ β -PbO₂ anode. Effect of parameters and optimization using response surface methodology. *Water Environ Res* 92(7):975–986
- Malakotian M, Asadipour A, Mohammadi Senjedkooch S (2016) A survey of the efficacy of calcium peroxide nanoparticles in the removal of reactive Red 198 from textile wastewater. *J Sabzevar Univ Med Sci* 23(1):110–121
- Méndez-Paz D, Omil F, Lema J (2005) Anaerobic treatment of azo dye Acid Orange 7 under fed-batch and continuous conditions. *Water Res* 39(5):771–778
- Mohan D, Pittman CU Jr (2006) Activated carbons and low cost adsorbents for remediation of tri- and hexavalent chromium from water. *J Hazard Mater* 137(2):762–811
- Moradiazad E, Adham D, Solimanzadeh H, Saghafipour A, Eghbal H (2019) The impact of climatic factors on spatial distribution of scorpion stings in Ardabil Province, North-West of Iran; 2012–2017. *Shiraz E-Med J*. <https://doi.org/10.5812/semj.69333>
- Moussavi G, Hosseini H, Alahabadi A (2013) The investigation of diazinon pesticide removal from contaminated water by adsorption onto NH₄Cl-induced activated carbon. *Chem Eng J* 214:172–179
- Nikzad S, Amooyi AA, Alinejad-Mir A (2019) Adsorption of diazinon from aqueous solutions by magnetic guar gum-montmorillonite. *Chem Data Collect* 20:100187
- Oller I, Malato S, Sánchez-Pérez J (2011) Combination of advanced oxidation processes and biological treatments for wastewater decontamination—a review. *Sci Total Environ* 409(20):4141–4166
- Ouazene N, Sahmoune MN (2010) Equilibrium and kinetic modeling of astrazon yellow adsorption by sawdust: effect of important parameters. *Int J Chem Reactor Eng*. <https://doi.org/10.2202/1542-6580.2413>
- Ouznadj ZB, Sahmoune MN, Mezenner NY (2016) Adsorptive removal of diazinon: kinetic and equilibrium study. *Desalin Water Treat* 57(4):1880–1889
- Ponnusami V, Krithika V, Madhuran R, Srivastava S (2007) Biosorption of reactive dye using acid-treated rice husk: factorial design analysis. *J Hazard Mater* 142(1–2):397–403
- Pourali P, Behzad M, Arfaeina H, Ahmadfazel A, Afshin S, Poureshgh Y, Rashtbari Y (2021) Removal of acid blue 113 from aqueous solutions using low-cost adsorbent: adsorption isotherms, thermodynamics, kinetics and regeneration studies. *Sep Sci Technol* 56(18):3079–3091
- Pourali P, Fazlzadeh M, Aaligadri M, Dargahi A, Poureshgh Y, Kakavandi B (2022) Enhanced three-dimensional electrochemical process using magnetic recoverable of Fe₃O₄@GAC towards furfural degradation and mineralization. *Arabian J Chem* 15(8):103980
- Pouretedal H, Sadegh N (2014) Effective removal of amoxicillin, cephalixin, tetracycline and penicillin G from aqueous solutions using activated carbon nanoparticles prepared from vine wood. *J Water Process Eng* 1:64–73
- Ramezani F, Kazemi B, Jebali A (2013) Biosynthesis of silver nanoparticles by *Leishmania* sp. *New Cell Mol Biotechnol J* 3(9):107–111
- Rashtbari Y, Abazari M, Arfaeina L, Gholizadeh A, Afshin S, Poureshgh Y, Alipour M (2021) The optimization of reactive black 5 dye removal in the sono-catalytic process combined with local yellow montmorillonite and hydrogen peroxide using response surface methodology from aqueous solutions. *Biomass Convers Biorefinery*. <https://doi.org/10.1007/s13399-021-01773-7>
- Rashtbari Y, Afshin S, Hamzezhadeh A, Abazari M, Poureshgh Y, Fazlzadeh M (2019) Application of powdered activated carbon coated with zinc oxide nanoparticles prepared using a green synthesis in removal of Reactive Blue 19 and Reactive Black-5: adsorption isotherm and kinetic models. *Desalin Water Treat* 179:354–367
- Rashtbari Y, Afshin S, Hamzezhadeh A, Abazari M, Poureshgh Y, Fazlzadeh M (2020a) Application of powdered activated carbon coated with zinc oxide nanoparticles prepared using a green synthesis in removal of Reactive Blue 19 and Reactive Black-5: adsorption isotherm and kinetic models. *Desalin Water Treat* 179:354–367
- Rashtbari Y, Afshin S, Hamzezhadeh A, Gholizadeh A, Ansari FJ, Poureshgh Y, Fazlzadeh M (2022) Green synthesis of zinc oxide nanoparticles loaded on activated carbon prepared from walnut peel extract for the removal of Eosin Y and Erythrosine B dyes from aqueous solution: experimental approaches, kinetics models, and thermodynamic studies. *Environ Sci Pollut Res* 29(4):5194–5206
- Rashtbari Y, Américo-Pinheiro JHP, Bahrami S, Fazlzadeh M, Arfaeina H, Poureshgh Y (2020b) Efficiency of zeolite coated with zero-valent iron nanoparticles for removal of humic acid from aqueous solutions. *Water Air Soil Pollut* 231(10):1–15
- Rashtbari Y, Hazrati S, Azari A, Afshin S, Fazlzadeh M, Vosoughi M (2020c) A novel, eco-friendly and green synthesis of PPAC-ZnO and PPAC-nZVI nanocomposite using pomegranate peel: cephalixin adsorption experiments, mechanisms, isotherms and kinetics. *Adv Powder Technol* 31(4):1612–1623
- Rivera-Utrilla J, Sánchez-Polo M, Prados-Joya G, Ferro-García M, Bautista-Toledo I (2010) Removal of tinidazole from waters by using ozone and activated carbon in dynamic regime. *J Hazard Mater* 174(1–3):880–886
- Ryoo KS, Jung SY, Sim H, Choi J-H (2013) Comparative study on adsorptive characteristics of diazinon in water by various adsorbents. *Bull Korean Chem Soc* 34(9):2753–2759
- Saeidi M, Naeimi A, Komeili M (2016) Magnetite nanoparticles coated with methoxy polyethylene glycol as an efficient adsorbent of diazinon pesticide from water. *Adv Environ Technol* 2(1):25–31
- Samadi MT, Khodadadi M, Rahmani AR, Allahresani A, Saghi MH (2010) Comparison of the efficiency of simultaneous application of UV/O₃ for the removal of organophosphorus and carbamate pesticides in aqueous solutions. *J Water Wastewater; Ab Va Fazilab (in Persian)* 21(1):69–75
- Samarghandi M, Rahmani A, Asgari G, Ahmadidoost G, Dargahi A (2018) Photocatalytic removal of cefazolin from aqueous solution by AC prepared from mango seed+ ZnO under uv irradiation. *Global NEST J* 20(2):399–407
- Samarghandi MR, Ansari A, Dargahi A, Shabanloo A, Nematollahi D, Khazaei M, Nasab HZ, Vaziri Y (2021) Enhanced electrocatalytic degradation of bisphenol A by graphite/ β -PbO₂ anode in a three-dimensional electrochemical reactor. *J Environ Chem Eng* 9(5):106072

- Shahrokhi-Shahraki R, Benally C, El-Din MG, Park J (2021) High efficiency removal of heavy metals using tire-derived activated carbon vs commercial activated carbon: insights into the adsorption mechanisms. *Chemosphere* 264:128455
- Shu H-Y, Chang M-C, Yu H-H, Chen W-H (2007) Reduction of an azo dye Acid Black 24 solution using synthesized nanoscale zerovalent iron particles. *J Colloid Interface Sci* 314(1):89–97
- Shu YR, Ji B, Cui BH, Shi YT, Wang J, Hu M, Luo SY, Guo DB (2020) Almond shell-derived, Biochar-supported, nano-zero-valent iron composite for aqueous hexavalent chromium removal: performance and mechanisms. *Nanomaterials* 10(2):198
- Videira RA, Antunes-Madeira MC, Lopes, V.n.I. and Madeira, V.t.M. (2001) Changes induced by malathion, methylparathion and parathion on membrane lipid physicochemical properties correlate with their toxicity. *Biochimica Et Biophys Acta (BBA) Biomembr* 1511(2):360–368
- Xiong Z, Cheng X, Sun D (2011) Pretreatment of heterocyclic pesticide wastewater using ultrasonic/ozone combined process. *J Environ Sci* 23(5):725–730
- Xu W, Zhao Q, Wang R, Jiang Z, Zhang Z, Gao X, Ye Z (2017) Optimization of organic pollutants removal from soil eluent by activated carbon derived from peanut shells using response surface methodology. *Vacuum* 141:307–315
- Zhang H, Duan L, Zhang Y, Wu F (2005) The use of ultrasound to enhance the decolorization of the CI acid orange 7 by zero-valent iron. *Dyes Pigm* 65(1):39–43
- Zhang XR, Yan L, Liu JF, Zhang ZY, Tan CH (2019) Removal of different kinds of heavy metals by novel PPG-nZVI Beads and their application in simulated stormwater infiltration facility. *Appl Sci Basel* 9(20):4213
- Zohair A (2001) Behaviour of some organophosphorus and organochlorine pesticides in potatoes during soaking in different solutions. *Food Chem Toxicol* 39(7):751–755
- Zolgharnein J, Shahmoradi A, Ghasemi JB (2013) Comparative study of Box-Behnken, central composite, and Doehlert matrix for multivariate optimization of Pb (II) adsorption onto Robinia tree leaves. *J Chemom* 27(1–2):12–20

Publisher's Note Springer Nature remains neutral with regard to jurisdictional claims in published maps and institutional affiliations.